n°1239

Analytical Prediction of Chatter Stability in Milling—Part I: General Formulation

E. Budak[1]

Y. Altintaş

Department of Mechanical Engineering,
The University of British Columbia,
Vancouver, B.C. Canada V6T 1Z4

A new analytical method of chatter stability prediction in milling is presented. A general formulation for the dynamic milling system is developed by modeling the cutter and workpiece as multi-degree of freedom structures. The dynamic interaction between the milling cutter and workpiece is modeled considering the varying dynamics in the axial direction. The dynamic milling forces are governed by a system of periodic differential equations with delay whose stability analysis leads to an analytical solution for chatter stability limit in milling. The model can be used to determine the chatter free axial and radial depth of cuts without resorting to time domain simulations.

1 Introduction

Machine tool chatter vibrations are the self-excited oscillations of the cutting tool and the workpiece. If the closed-loop machining system, which includes machine tool-cutter dynamics and the dynamic cutting process, becomes unstable, the excessive vibrations of the cutter and workpiece result in poor surface finish and dimensional accuracy, chipping of the cutter teeth, and may damage the workpiece and machine tool. In general, conservative material removal rates, which cause reduced productivity, are used to avoid chatter vibrations.

Although in the early stage of the machining chatter research, the presence of negative damping was considered as the only source of chatter, it was later recognized by Tobias (1958) and Tlusty (1963) that the most powerful sources of self excitation, *regeneration* and *mode coupling*, are associated with the structural dynamics of the machine tool and the feedback between the subsequent cuts. Tobias and Fiswick (1958) combined the dynamics of the cutting process and the machine tool structure, and included the process damping and stiffness in their chatter stability model. Parallel to Tobias, Tlusty and Polacek (1963) presented a practical stability law for orthogonal cutting systems, where the chatter free axial depth of cut can be identified as a function of structural dynamics of the machine tool—workpiece and cutting stiffness oriented in the direction of cut. Merritt (1965) used feedback control theory to develop stability lobe diagrams for regenerative chatter. These fundamental studies are applicable to orthogonal cutting, where the direction of the cutting force, chip thickness and structural dynamics do not change with time. On the other hand, the stability analysis of milling is complicated by the rotating tool, multiple cutting teeth, periodically varying cutting forces and chip load directions and multi degree of freedom structural dynamics. The directional coefficients (direction cosines of the cutting force and the oriented transfer functions in the chip thickness direction) vary as the cutter rotates which has been the main difficulty in milling stability analysis. In the past, various approximations were used in order to simplify the problem so that standard stability theories can be applied. In the early milling stability analysis, Tlusty (1967) applied his orthogonal cutting-stability formulation by considering an average direction and average number of flutes in cut. Opitz et al. (1968, 1970) approximated the periodic coefficients with their average values. Later Tlusty et al. (1981, 1986, 1983) showed that milling stability conditions can be predicted by considering nondirectional and velocity dependent process damping mechanisms in the time domain simulations. Altintas et al. (1992) presented time domain simulation model for a complex plate milling system with multi-degree-of-freedom structural dynamics. They considered stiffness and damping of the process by modeling ploughing and indentation of the cutting edges during vibrations. The time domain simulations have to be repeated numerous times, and care must be taken to avoid numerical instabilities in calculating very small displacements.

The analytical approaches to the prediction of chatter stability in metal cutting has gained momentum for the process planning of machining operations at high speeds (Minis and Yanushevsky, 1990; Chen et al., 1993). The first comprehensive theoretical analysis of milling stability has been performed by Sridhar et al. (1968). They formulated the dynamic milling forces for a straight tooth cutter. Because of the periodic and delay terms, they used a stability algorithm which is based on the numerical evaluation of the system's state transition matrix. There exist several analytical methods to study the stability of periodic or delayed (difference) equations. Hill's equation is the procedure of the infinite determinant which utilizes the Floquet's theorem and the Fourier series expansion of the periodic coefficients (Magnus and Winkler, 1966). On a two-degree-of-freedom cutter model with point contact, Minis and Yanushevsky (1990, 1993) successfully used this procedure in solving the milling stability equation, which is a noted step forward from Sridhar's (1968b) formulation of the expression. They used the Nyquist stability criterion to determine the stability limits. Although the algorithm depends on the numerical evaluation of the stability limits, i.e., chatter free axial depth of cuts, at different spindle speeds, their work provided more comprehensive modelling in determining the stability limits in milling. Lee et al. (1991a, 1991b) also used the Nyquist criterion to determine the stability limits, but using numerical methods.

In this paper, an alternative analytical stability model is presented. The milling cutter and workpiece are modeled as multi degree-of-freedom structures. The dynamic interaction in the cutting zone is modeled by including the variations in the cutter and workpiece dynamics in axial direction, unlike the point contact models used in the previous analysis. This extension is not only for the completeness of the developed dynamic milling model. It is demonstrated with numerical examples that it can also increase the accuracy of the predictions for the cases where

[1] Currently with Pratt and Whitney Canada, 1000 Marie-Victorin, Longueuil, Quebec, Canada J4G 1A1.

Contributed by the Dynamic Systems and Control Division for publication in the JOURNAL OF DYNAMIC SYSTEMS, MEASUREMENT, AND CONTROL. Manuscript received by the DSCD January 4, 1995. Associate Technical Editor: Yoram Koren.

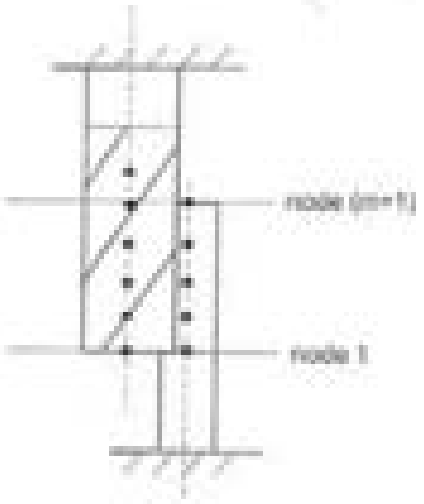

Fig. 1 Model of the cutter and workpiece for chatter analysis

the workpiece is highly flexible. Some practical examples for these cases are peripheral milling of thin webs, compressor and fan blades (Wu, 1995) and other thin walled workpieces (Altintas et al., 1992) with long axial depth of cut. The stability analysis of the system is performed by applying periodic system theory, and considering the physics of dynamic milling. It is shown that some major simplifications in the formulation are possible by interpreting the physical meanings of the terms in the stability formulation. This analysis results in analytical relations for the chatter frequency and chatter stability limit which are used to generate the stability diagrams. The comprehensive formulation is general for multi-degree-of-freedom systems in milling, but simplified for most common face and peripheral milling systems, which have reduced dominant dynamics at the tool-workpiece contact point, as presented in Part II of the paper as applications (Budak and Altintas).

Henceforth, the paper is organized as follows. In Section II, the modeling of the dynamic milling system is given, and the dynamic milling forces are formulated for the general case where structural dynamics in three directions are considered for helical end milling operations. The stability analysis of the dynamic milling process is performed in Section III. Based on the developed stability formulation, the expressions between the chatter frequency and the chatter limit are derived in Section IV. The analytical model predictions are verified by experimental and numerical results on an end milling example at the end of the paper. The application of the general formulation to some common milling systems is demonstrated in the second part of the paper.

II Formulation of the Dynamic Milling Forces

Modeling of the Dynamic Milling System. A point contact between the milling cutter and the workpiece has been considered in the previous milling stability studies. In these, the cutter is modeled as a two-degree-of-freedom structure which is lumped at the tip of the tool and the variation of the dynamics in the axial direction is neglected. This is a satisfactory model for most of the milling systems where the chatter free axial depth of cuts are very small compared to the overall length of the cutter. However, this variation can be important when the workpiece has a vibration mode with a very steep variation at some points along the axial direction (e.g., a thin cantilevered plate).

In the present analysis, the cutter and workpiece are divided into a number of elements in the axial direction in order to model the dynamic interaction between them accurately. The discrete modeling of the cutter and workpiece, as shown in Fig. 1, is very convenient for modal identification of the cutter and workpiece dynamics, and the dynamic milling force formulation as it will be shown later. The cutter and workpiece dynamics are lumped at the $(m + 1)$ equally spaced nodes along the axial direction. The cutter dynamics are assumed to be constant along the feed direction whereas the workpiece dynamics can be variable in which case the analysis should be repeated at a number of different locations.

The milling dynamics can be represented by

$$[M]\{\ddot{x}\}(t) + [C]\{\dot{x}\}(t) + [K]\{x\}(t) = \{F\} \qquad (1)$$

where $\{x\}(t)$ is the modal displacements of workpiece and cutter whose mass, damping and stiffness matrices are represented by $[M]$, $[C]$, $[K]$. $\{F\}$ contains the static and dynamic milling forces which are proportional to the static and dynamic, or regenerative, chip thickness, as formulated in the following section.

Dynamic-Regenerative Chip Thickness Model. Figure 2 shows a cross-section of an end mill tooth (j) vibrating and removing a wavy surface cut by the previous tooth $(j + N)$. u_j and v_j are the instantaneous tangential and normal directions at the tip of tooth j, and they can be expressed in terms of the fixed coordinate system x and y as follows:

$$u_j = -x \cos\phi_j(z) + y \sin\phi_j(z),$$
$$v_j = -x \sin\phi_j(z) - y \cos\phi_j(z) \qquad (2)$$

where $\phi_j(z) = \phi + j\phi_p - k_\phi z$, $k_\phi = \tan\psi/R$, $\phi_p = 2\pi/N$. N is the number of teeth on the cutter, ϕ_p is the cutter pitch angle, ψ is the helix angle, R is the cutter radius and $\phi = \Omega t$ is the rotation angle of the end mill (measured with respect to tooth number $j = 0$ from the positive y axis), Ω being the rotational speed of the cutter in (rad/s). In dynamic milling, a vibrating cutter tooth removes the modulated surface left by the previous tooth, in addition to the static chip load defined by the feed per tooth s_t. Then, the chip thickness can be written as a summation of the static and the regenerative parts as,

$$h_j(\phi, z) = (v_0^c - v_0^w) - (v_0 - v_0) + s_t \sin\phi_j(z) \qquad (3)$$

where v_0, v_0 and v_0^c, v_0^w are the dynamic displacements of the cutter and workpiece in the v direction, for current and previous tooth passes (for the rotation angle of the cutter ϕ, at the axial depth z), respectively. According to the reference system shown in Fig. 2, the current cutter displacements in the positive v_j direction decrease the chip thickness, whereas it is increased by the positive cutter displacements in the previous pass. In this stage of the formulation, the cutter and workpiece deflections

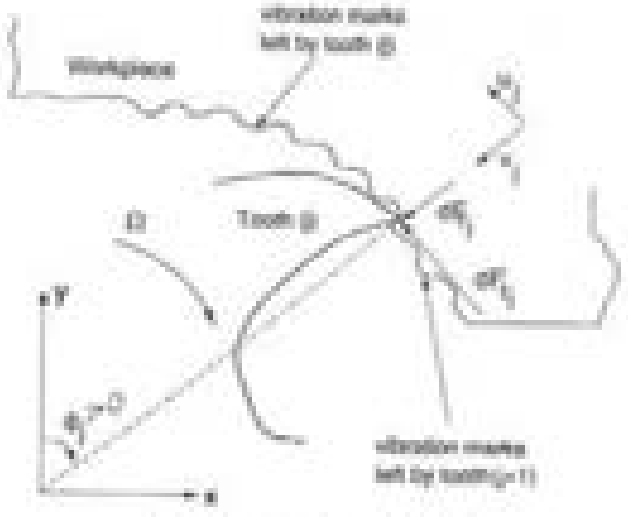

Fig. 2 Dynamic milling process

are considered to be in the $+y$ direction, although they either deflect toward or apart from each other, which will be considered when dynamic displacement-milling force relations are introduced. Substituting for the rotating coordinates from Eq. (2), the following is obtained:

$$h(\phi, z) = [(x_s - x_s^*) - (x_w - x_w^*)] \sin \phi(z) + [(y_s - y_s^*) - (y_w - y_w^*)] \cos \phi(z) + s \sin \phi(z) \quad (4)$$

where x_s, y_s and x_w, y_w are the cutter and workpiece displacements in the current tooth pass in the x and y directions (for the rotation angle of the cutter ϕ and at the axial depth z), respectively. Similarly, x_s^*, y_s^* and x_w^*, y_w^* are cutter and the workpiece displacements imprinted on the surface by the previous tooth at the same point.

Differential Dynamic Milling Forces. The milling forces in the x and y directions are considered only, since the spindle and the cutter are quite rigid in the z direction. The differential tangential (dF_t) and radial (dF_r) cutting forces (Fig. 2) on a tooth for an infinitesimal axial thickness of dz can be expressed as follows:

$$dF_t(\phi, z) = K_t A(\phi, z) g(\phi, z) dz, \quad dF_r(\phi, z) = K_r dF_t \quad (5)$$

where K_t and K_r are the tangential and radial milling force coefficients which are experimentally determined for a cutter-workpiece material pair. $g(\phi(z))$ is a unit pulse function which determines whether the tooth is in or out of cut, i.e.,

$$\left.\begin{aligned} g(\phi(z)) &= 1 \quad \phi_{st} < \phi(z) < \phi_{ex} \\ g(\phi(z)) &= 0 \quad \phi(z) < \phi_{st} \quad \text{or} \quad \phi(z) > \phi_{ex} \end{aligned}\right\} \quad (6)$$

where ϕ_{st} and ϕ_{ex} are the start and exit angles of a tooth to and from the cut, respectively. According to the coordinate frame shown in Fig. 3, $\phi_{st} = 0$ always for up milling and ϕ_{ex} depends on the radial depth of cut, whereas $\phi_{ex} = \pi$ always for down milling. The tangential and radial forces can be resolved in the feed (x) and normal (y) directions as follows:

$$dF_x(\phi, z) = [-dF_t(\phi, z) \cos \phi(z) - dF_r(\phi, z) \sin \phi(z)] g(\phi(z))$$

$$dF_y(\phi, z) = [dF_t(\phi, z) \sin \phi(z) - dF_r(\phi, z) \cos \phi(z)] g(\phi(z)) \quad (7)$$

Substituting Eqs. (4) and (5) into (7), the following explicit form is obtained for the differential milling forces:

$$dF_x(\phi, z) = -K_t[\cos \phi(z) + K_r \sin \phi(z)] \times [(x_s - x_s^*) - (x_w - x_w^*)] \sin \phi(z) + [(y_s - y_s^*) - (y_w - y_w^*)] \cos \phi(z) + s \sin \phi(z)] g(\phi(z)) a dz$$

$$dF_y(\phi, z) = K_t[\sin \phi(z) - K_r \cos \phi(z)] \times [(x_s - x_s^*) - (x_w - x_w^*)] \sin \phi(z) + [(y_s - y_s^*) - (y_w - y_w^*)] \cos \phi(z) + s \sin \phi(z)] g(\phi(z)) a dz \quad (8)$$

Total Dynamic Milling Forces. The differential dynamic milling forces are integrated within an element i to determine the elemental milling forces for the flute j as:

$$F_x(i) = \int_{z_i}^{z_{i+1}} dF_x(\phi, z) dz, \quad F_y(i) = \int_{z_i}^{z_{i+1}} dF_y(\phi, z) dz \quad (9)$$

where z_i and z_{i+1} are the lower and upper z coordinates of the axial element (i). After the integration, Eq. (9) can be arranged as follows:

$$F_x(i) = F_x^s(i) - K_t[C_{xc}(i) + K_r C_{xy}(i) + C_{yc}(i) + K_r C_{ys}(i)]$$

$$F_y(i) = F_y^s(i) + K_t[C_{xc}(i) - K_r C_{xy}(i) + C_{ys}(i) - K_r C_{yc}(i)] \quad (10)$$

$F_x^s(i)$ and $F_y^s(i)$ in Eq. (10) are the milling forces generated within the axial element i due to static component of the chip thickness ($s \sin \phi_j(z)$):

$$F_x^s(i) = \frac{K_t a}{4 k_b}[-\cos 2\phi_j(z) + K_r(2\phi_j(z) - \sin 2\phi_j(z))]_{z_i}^{z_{i+1}}$$

$$F_y^s(i) = \frac{K_t a}{4 k_b}[2\phi_j(z) - \sin 2\phi_j(z) + K_r \cos 2\phi_j(z)]_{z_i}^{z_{i+1}} \quad (11)$$

In order to simplify the formulation, the deflections will be assumed to remain constant within each element. Furthermore, the helix angle within each element will be neglected (straight tooth) which also means that the unit pulse function $g(\phi_j(z))$ is invariant within the element. However, it should be noted that the helix angle is still considered between the elements along the axial direction, and the accuracy can be controlled by selecting shorter elements. Then, the coefficients in Eq. (10) are obtained as

$$C_{xc}(i) = \tfrac{1}{2} a \Delta z K_t \Delta x(i) g(i) \sin 2\phi_j(z)$$

$$C_{xs}(i) = \tfrac{1}{2} a \Delta z K_t \Delta x(i) g(i) [1 - \cos 2\phi_j(i)]$$

$$C_{yc}(i) = \tfrac{1}{2} a \Delta z K_t \Delta y(i) g(i) [1 + \cos 2\phi_j(i)]$$

$$C_{ys}(i) = \tfrac{1}{2} a \Delta z K_t \Delta y(i) g(i) \sin 2\phi_j(i) \quad (12)$$

where

$$\Delta x(i) = [x_s(i) - x_s^*(i)] - [x_w(i) - x_w^*(i)]$$

$$\phi_j(i) = \phi_j(\phi, z_i)$$

$$g(i) = g(\phi_j(z_i))$$

$$\Delta z = z_{i+1} - z_i = a/m$$

and m is the number of axial elements, a is the axial depth of cut, $[x_s(i), y_s(i)]$ and $[x_w(i), y_w(i)]$ are the nodal displacements of the cutter and the workpiece for the considered rotational angle of the cutter, and $[x_s^*(i), y_s^*(i)]$ and $[x_w^*(i), y_w^*(i)]$ are the nodal displacements in the previous tooth pass at the same immersion point.

Substituting Eq. (12) into (10) the following is obtained for the nodal dynamic milling forces:

$$\begin{Bmatrix} F_x(i) \\ F_y(i) \end{Bmatrix} = \begin{Bmatrix} F_x^s(i) \\ F_y^s(i) \end{Bmatrix} + a \begin{bmatrix} a_{xx}(i) & a_{xy}(i) \\ a_{yx}(i) & a_{yy}(i) \end{bmatrix} \begin{Bmatrix} \Delta x(i) \\ \Delta y(i) \end{Bmatrix} \quad (13)$$

where

$$a = \tfrac{1}{2} \Delta z K_t \quad (14)$$

In Eq. (13), the matrix elements $a_{xx}, \ldots, a_{yy}$ which relate the dynamic displacements to the dynamic milling forces will be called directional dynamic milling coefficients and are given as:

$$a_{xx}(i) = -g[\sin 2\phi_j(i) + K_r(1 - \cos 2\phi_j(i))]$$

$$a_{xy}(i) = -g[(1 + \cos 2\phi_j(i)) + K_r \sin 2\phi_j(i)]$$

$$a_{yx}(i) = g[(1 - \cos 2\phi_j(i)) - K_r \sin 2\phi_j(i)]$$

$$a_{ij}(j) = \frac{a}{2}\left[\sin 2\phi_j(j) - K_t(1 + \cos 2\phi_j(j))\right] \quad (15)$$

The total milling forces in each differential element (j) can be obtained by summing up the cutting forces on each flute:

$$F_x(j) = \sum_{j=0}^{N-1} F_{xj}(j), \quad F_y(j) = \sum_{j=0}^{N-1} F_{yj}(j) \quad (16)$$

where N is the number of flutes on the cutter. It can be seen from Eqs. (2) and (15) that the total directional dynamic milling coefficients are periodic with the pitch angle $\phi_p = 2\pi/N$. Equation (13) can be written for every axial element, and when they are combined, the following matrix equation is obtained for the whole structure:

$$\begin{Bmatrix} \{F_x\} \\ \{F_y\} \end{Bmatrix} = \begin{Bmatrix} \{F_x^0\} \\ \{F_y^0\} \end{Bmatrix} + a\begin{bmatrix} [a_{xx}] & [a_{xy}] \\ [a_{yx}] & [a_{yy}] \end{bmatrix}\begin{Bmatrix} \{\Delta x\} \\ \{\Delta y\} \end{Bmatrix} \quad (17)$$

or in more compact form

$$\{F\} = \{F^0\} + a[A(t)]\{\Delta\} \quad (18)$$

where

$$\{\Delta\} = \begin{Bmatrix} \{\Delta x\} \\ \{\Delta y\} \end{Bmatrix} \quad (19)$$

The force and the displacement vectors contain the elemental force and displacements, e.g., $\{F_x\}^T = \{F_x(1), F_x(2), \ldots, F_x(m)\}$. $[a_{xx}]$, $[a_{xy}]$, $[a_{yx}]$ and $[a_{yy}]$ are diagonal matrices with elemental values of $a_{xx}(1), a_{xx}(2), \ldots,$ in the diagonal, i.e.,

$$\left.\begin{aligned} [a_{xx}]_{jj} &= a_{xx}(j) \quad j = i \\ [a_{xx}]_{ji} &= 0 \qquad j \neq i \end{aligned}\right\} \quad (20)$$

where

$$a_{xx}(j) = \sum_{j=0}^{N-1} a_{xxj}(j) \quad (21)$$

$[A(t)]$ will be referred to as the directional dynamic milling coefficient matrix which is periodic at the tooth passing frequency $\omega_t = N\Omega$. Equation (17) defines the dynamic milling forces by including the effects of the cutter rotation, helix angle and the variation in the cutter and workpiece dynamics along the axial direction.

III Stability Analysis of Dynamic Milling

The dynamic milling forces are generated by the dynamic displacements of the tool and workpiece. Therefore, the static components of the milling forces, $\{F_x^0\}$ and $\{F_y^0\}$ (which are due to the mean chip thickness or the static load), are not to be considered in the stability analysis. Then Eq. (18) becomes:

$$\{F\} = a[A(t)]\{\Delta\} \quad (22)$$

where

$$\{\Delta\} = \{\{x_c\} - \{x^0\}\} - \{\{x_w\} - \{x^0\}\} \quad (23)$$

$\{x_c\} = [\{x_c\}\{y_c\}]^T$ and $\{x_w\} = [\{x_w\}\{y_w\}]^T$ are the cutter and workpiece displacements, respectively. The directional dynamic milling coefficient matrix is periodic at tooth passing period $T = 2\pi/\omega_t$, and can be expanded into Fourier series:

$$[A(t)] = \sum_{r=-\infty}^{\infty} [A_r]e^{ir\omega_t t}, \quad [A_r] = \frac{1}{T}\int_0^T [A(t)]e^{-ir\omega_t t}dt \quad (24)$$

where the tooth passing frequency is $\omega_t = N\Omega$. The periodic terms in $[A(t)]$ are due to the time varying directional milling coefficients between the local chip thickness directions and the milling forces.

When the displacement-force relations are substituted in Eqs. (22) and (23), a set of equations, identified as *linear periodic-differential difference equations*, are obtained (Budak, 1994). The *difference* terms are due to the delay between the subsequent teeth.

In milling, the vibrations at ω_c occur due to two main reasons. First, the cutting forces are periodic in tooth passing frequency ω_t, and they cause forced vibrations which are excluded from the stability analysis as they are proportional to the mean chip thickness. Second, the dynamic milling system, which is modeled as a linear dynamic system in Eq. (22), must respond to the periodic variations in the directional dynamic milling coefficients contained in the matrix $[A(t)]$, which relates the dynamic displacements to the dynamic milling forces. On the other hand, it is well known from the experimental observations that the chatter vibrations occur at a frequency which is very close to one of the structural frequencies of the cutting system. Also, the amplitude of vibrations at the chatter frequency ω_c are much higher than forced vibrations which occur at the harmonics of the tooth passing frequency ω_t. In accordance with these observations, two separate formulations are given in the following: one which includes the effect of variations in the directional dynamic milling coefficients by considering the harmonic terms in $[A(t)]$: multi-frequency solution, and one by considering the vibrations at the chatter frequency only, i.e., by neglecting the harmonic terms and retaining only the average value in the Fourier expansion of $[A(t)]$: single frequency solution. The numerical examples in this and second part of the paper (Budak and Altintas) show that the results obtained by the two separate formulations are very close to each other. This is expected as the amplitude of the vibrations at the chatter frequency is always dominant.

Multi-Frequency Solution. If the periodic components of $[A(t)]$ are considered in the solution, then the response of the dynamic forces to these variations should also be included:

$$\{F\} = e^{i\omega_c t}\sum_{k=-\infty}^{\infty} \{F_k\}e^{ik\omega_t t} = \sum_{k=-\infty}^{\infty} \{F_k\}e^{i(\omega_c + k\omega_t)t} \quad (25)$$

Hence, the vibrations at the chatter frequency is superimposed on the ones at the integer multiples of the tooth frequency. Note that Eq. (25) is equivalent to the Floquet's theorem (Magnus and Winkler, 1966). Then, by superposition, the dynamic displacements can be written as follows:

$$\{x_c\} = \sum_{k=-\infty}^{\infty} [G_c(i\omega_c + ik\omega_t)]\{F_k\}e^{i(\omega_c + k\omega_t)t}$$

$$\{x_w\} = -\sum_{k=-\infty}^{\infty} [G_w(i\omega_c + ik\omega_t)]\{F_k\}e^{i(\omega_c + k\omega_t)t} \quad (26)$$

$[G_c(i\omega_c)]$ and $[G_w(i\omega_c)]$ are the structural transfer function matrices of the cutter and workpiece in the cutting zone:

$$[G_p(i\omega_c)] = \begin{bmatrix} [G_{xx_p}(i\omega_c)] & [G_{xy_p}(i\omega_c)] \\ [G_{yx_p}(i\omega_c)] & [G_{yy_p}(i\omega_c)] \end{bmatrix} (p = c, w) \quad (27)$$

where $[G_{xx_p}(i\omega_c)]$ and $[G_{yy_p}(i\omega_c)]$ are the direct transfer function matrices in x and y directions, and $[G_{xy_p}(i\omega_c)]$ and $[G_{yx_p}(i\omega_c)]$ are the cross transfer functions.

The phase difference between the vibration waves of two successive teeth is $\omega_c T$, where T is the tooth period. The dynamic displacements of the cutter and workpiece in the preceding tooth period can be expressed as follows:

$$\{x_c^0\} = \{x_c(t - T)\} = e^{-i\omega_c T}\{x_c\},$$

$$\{x_w^0\} = \{x_w(t - T)\} = e^{-i\omega_c T}\{x_w\} \quad (28)$$

Then, $\{\Delta\}$ in Eq. (23) becomes:

$$\{\Delta\} = (\{r_c\} - \{r_w\})(1 - e^{-i\omega_c T}) \qquad (29)$$

Substituting into (22) the following is obtained:

$$\sum_{k=-\infty}^{\infty} \{F_k\} e^{i(\omega_c + k\omega_T)t} = a(1 - e^{-i\omega_c T})[A(t)]$$

$$\times \sum_{k=-\infty}^{\infty} [G(i\omega_c + ik\omega_T)]\{F_k\} e^{i(\omega_c + k\omega_T)t}$$

$$\sum_{k=-\infty}^{\infty} \{F_k\} e^{ik\omega_T t} = a(1 - e^{-i\omega_c T}) \sum_{r=-\infty}^{\infty} [A_r] e^{ir\omega_T t}$$

$$\times \sum_{k=-\infty}^{\infty} [G(i\omega_c + ik\omega_T)]\{F_k\} e^{ik\omega_T t}$$

$$\sum_{k=-\infty}^{\infty} \{F_k\} e^{ik\omega_T t} = a(1 - e^{-i\omega_c T})$$

$$\times \sum_{r=-\infty}^{\infty} \sum_{k=-\infty}^{\infty} [A_r][G(i\omega_c + ik\omega_T)]\{F_k\} e^{i(r+k)\omega_T t} \qquad (30)$$

If both sides of the equation are multiplied by $1/T e^{-ip\omega_T t}$ and integrated from 0 to T, by using the orthogonality principle the following is obtained:

$$\{F_p\} = a(1 - e^{-i\omega_c T}) \sum_{k=-\infty}^{\infty} [A_{p-k}][G(i\omega_c + ik\omega_T)]\{F_k\}$$

$$(p = 0, \pm 1, \pm 2, \ldots) \qquad (31)$$

Equation (31) can be written in the following infinite matrix form:

$$\begin{Bmatrix} \{F_0\} \\ \{F_1\} \\ \{F_{-1}\} \\ \vdots \end{Bmatrix} = a(1 - e^{-i\omega_c T})$$

$$\times \begin{bmatrix} [A_0][G(i\omega_c)] & [A_{-1}][G(i\omega_c + i\omega_T)] & \cdots \\ [A_1][G(i\omega_c)] & [A_0][G(i\omega_c + i\omega_T)] & \cdots \\ [A_{-1}][G(i\omega_c)] & [A_{-2}][G(i\omega_c + i\omega_T)] & \cdots \\ \vdots & \vdots & \ddots \end{bmatrix}$$

$$\times \begin{Bmatrix} \{F_0\} \\ \{F_1\} \\ \{F_{-1}\} \\ \vdots \end{Bmatrix} \qquad (32)$$

Equation (32) has nontrivial solutions if the determinant is zero:

$$\det [\delta_{pk}[I] - a(1 - e^{-i\omega_c T})[A_{p-k}][G(i\omega_c + ik\omega_T)]] = 0 \qquad (33)$$

where δ_{pk} is the Kronecker delta and $[I]$ is the $(2m \times 2m)$ identity matrix. Equation (33) defines an infinite determinant which is a characteristic of the periodic systems. The truncated version of this equation must be used to obtain approximate solutions. For the first-order approximation $p, k = 0, \pm 1$, the following truncated determinant is obtained:

$$\det \begin{bmatrix} [I] + \Lambda[A_0][G(i\omega_c)] & \Lambda[A_{-1}][G(i\omega_c + i\omega_T)] & \Lambda[A_1][G(i\omega_c - i\omega_T)] \\ \Lambda[A_1][G(i\omega_c)] & [I] + \Lambda[A_0][G(i\omega_c + i\omega_T)] & \Lambda[A_2][G(i\omega_c - i\omega_T)] \\ \Lambda[A_{-1}][G(i\omega_c)] & \Lambda[A_{-2}][G(i\omega_c + i\omega_T)] & [I] + \Lambda[A_0][G(i\omega_c - i\omega_T)] \end{bmatrix} = 0 \qquad (34)$$

where the eigenvalue $\Lambda = -a(1 - e^{-i\omega_c T})$.

Single Frequency Solution. The response of the dynamic milling system only at the chatter frequency is considered in the single frequency solution, which is a special case of the multi frequency formulation. Then, the cutter and workpiece displacements can be determined from:

$$\{r_c\} = [G_c(i\omega_c)]\{F\} e^{i\omega_c t},$$

$$\{r_w\} = -[G_w(i\omega_c)]\{F\} e^{i\omega_c t} \qquad (35)$$

$\{F\}$ is the amplitude of the dynamic milling forces in x and y directions:

$$\{F\} = \begin{Bmatrix} \{F_x\} \\ \{F_y\} \end{Bmatrix} \qquad (36)$$

Substituting Eqs. (35) and (29) into Eq. (22), the following is obtained:

$$\{F\} e^{i\omega_c t} = a(1 - e^{-i\omega_c T})[A_0][G(i\omega_c)]\{F\} e^{i\omega_c t} \qquad (37)$$

where $[G] = [G_c] + [G_w]$. $[A_0]$ is the averaged value of $[A(t)]$ in a tooth period, i.e., the constant term in the Fourier series expansion of $[A(t)]$ in Eq. (24):

$$[A_0] = \frac{1}{T} \int_0^T [A(t)] dt. \qquad (38)$$

The higher Fourier coefficients of $[A(t)]$ are neglected as the response of the dynamic milling forces, cutter and workpiece to the periodic variations of the directional milling coefficients are not considered in this case. Equation (37) has nontrivial solutions if the determinant is zero:

$$\det [[I] - a(1 - e^{-i\omega_c T})[A_0][G(i\omega_c)]] = 0 \qquad (39)$$

which is the characteristic equation of the closed-loop dynamic milling system with single frequency solution approximation.

Fourier Coefficients of $[A(t)]$. As described before, $[A_0]$ contains the mean values of the corresponding periodic directional milling coefficients:

$$[A_0] = \frac{1}{T} \int_0^T \sum_{j=0}^{N-1} [A(t)] dt = \frac{1}{T} \int_0^T \begin{bmatrix} [a_{xx}] & [a_{xy}] \\ [a_{yx}] & [a_{yy}] \end{bmatrix} dt \qquad (40)$$

where $[a_{xx}], \ldots, [a_{yy}]$ are diagonal matrices with the elemental directional coefficients in the main diagonal. Before evaluating the integral defined in Eq. (40), consider the following change of variables:

$$\phi_j(k) = \phi + j\phi_p - k_\beta z_k$$

$$= \Omega(t + jT) - k_\beta z_k = \Omega\tau_j - k_\beta z_k \qquad (41)$$

where $\tau_j = t + jT$ and Ω is the angular speed of the spindle in (rad/s). Then, Eq. (40) becomes:

$$[A_0] = \frac{1}{T} \sum_{j=0}^{N-1} \int_{jT}^{(j+1)T} [A(\tau_j)] d\tau_j = \frac{1}{T} \int_0^{NT} [A(\tau)] d\tau \qquad (42)$$

Turning back to angular domain by substituting $\phi_k = \Omega\tau_j - k_\beta z_k$ and $T = 2\pi/\Omega$ the following is obtained:

$$[A_0] = \frac{N}{2\pi}\int_{\phi_{st}}^{\phi_{ex}-\gamma_p\gamma_x}\begin{bmatrix}[a_{xx}(\phi_j)] & [a_{xy}(\phi_j)]\\ [a_{yx}(\phi_j)] & [a_{yy}(\phi_j)]\end{bmatrix}d\phi \quad (43)$$

The elements of the diagonal matrices $[a_{xx}],\ldots,[a_{yy}]$ are given in Eq. (15).

Note that all the elements of the matrices $[a_{xx}],\ldots,[a_{yy}]$ are nonzero only in the interval $(\phi_{st} - \phi_{ex})$. Then, the limits of integration become ϕ_{st} and ϕ_{ex}, independent of the element axial position z. Therefore, the elements in the diagonal of $[a_{xx}],\ldots,[a_{yy}]$ become equal to each other. Then, Eq. (43) takes the following form:

$$[A_0] = \frac{N}{2\pi}\begin{bmatrix}a_{xx}^{(0)}(\theta)[I] & a_{xy}^{(0)}(\theta)[I]\\ a_{yx}^{(0)}(\theta)[I] & a_{yy}^{(0)}(\theta)[I]\end{bmatrix} \quad (44)$$

where $[I]$ is the $m \times m$ identity matrix, and

$$a_{xx}^{(0)} = \frac{1}{2}[\cos 2\theta - 2K_r\theta + K_r \sin 2\theta]_{\phi_{st}}^{\phi_{ex}}$$

$$a_{xy}^{(0)} = \frac{1}{2}[-\sin 2\theta - 2\theta + K_r \cos 2\theta]_{\phi_{st}}^{\phi_{ex}}$$

$$a_{yx}^{(0)} = \frac{1}{2}[-\sin 2\theta + 2\theta + K_r \cos 2\theta]_{\phi_{st}}^{\phi_{ex}}$$

$$a_{yy}^{(0)} = \frac{1}{2}[-\cos 2\theta - 2K_r\theta - K_r \sin 2\theta]_{\phi_{st}}^{\phi_{ex}} \quad (45)$$

Then, the single frequency solution takes the following form:

$$\det\,[[I]_{2m} + \Lambda[G_0(i\omega_c)]] = 0 \quad (46)$$

where $\Lambda = -(N/2\pi)\alpha(1 - e^{-i\omega_c T})$, $[G_0]$ can be regarded as the oriented transfer function in milling and is given as follows:

$$[G_0(i\omega_c)] = \begin{bmatrix}a_{xx}^{(0)}[G_{xx}(i\omega_c)] + a_{xy}^{(0)}[G_{yx}(i\omega_c)] & a_{xx}^{(0)}[G_{xy}(i\omega_c)] + a_{xy}^{(0)}[G_{yy}(i\omega_c)]\\ a_{yx}^{(0)}[G_{xx}(i\omega_c)] + a_{yy}^{(0)}[G_{yx}(i\omega_c)] & a_{yx}^{(0)}[G_{xy}(i\omega_c)] + a_{yy}^{(0)}[G_{yy}(i\omega_c)]\end{bmatrix} \quad (47)$$

where $[G_{xx}] = [G_{xx}] + [G_{xy}]$.

The procedure to obtain the higher Fourier coefficients is very similar to the one followed for $[A_0]$. The qth Fourier series coefficient of $[A(t)]$ is defined by

$$[A_q] = \frac{1}{T}\int_0^T [A(t)]e^{-iq\omega t}dt \quad (48)$$

Similar to the result obtained in Eq. (43), Eq. (48) takes the following form after the substitution of θ:

$$[A_q] = \frac{N}{2\pi}\int_{\phi_{st}}^{\phi_{ex}} [A(\theta)]e^{-iq\theta}d\theta \quad (49)$$

As in the case of zero order approximation, $[A_q]$ becomes independent of the axial position (or element number). Using trigonometric identities, the following general form for the coefficients $a_{xx},\ldots,a_{yy}$ are obtained:

$$a_{xx}^{(q)} = \frac{i}{2}[-c_q K_r e^{-iq\theta} + c_q e^{-i\theta} - c_q e^{i\theta}]_{\phi_{st}}^{\phi_{ex}}$$

$$a_{xy}^{(q)} = \frac{1}{2}[-c_q K_r e^{-iq\theta} + c_q e^{-i\theta} + c_q e^{i\theta}]_{\phi_{st}}^{\phi_{ex}}$$

$$a_{yx}^{(q)} = \frac{1}{2}[c_q K_r e^{-iq\theta} + c_q e^{-i\theta} + c_q e^{i\theta}]_{\phi_{st}}^{\phi_{ex}}$$

$$a_{yy}^{(q)} = \frac{i}{2}[-c_q K_r e^{-iq\theta} - c_q e^{-i\theta} + c_q e^{i\theta}]_{\phi_{st}}^{\phi_{ex}} \quad (50)$$

where

$$p_1 = 2 + Nq, \quad p_2 = 2 - Nq$$

$$c_q = \frac{2}{Nq}, \quad c_1 = \frac{K_r - i}{p_1}$$

$$c_2 = \frac{K_r + i}{p_2} \quad (51)$$

Also, $a_{xx}^{(-q)}, a_{xy}^{(-q)}, a_{yx}^{(-q)}, a_{yy}^{(-q)}$ are equal to the complex conjugates of $a_{xx}^{(q)}, a_{xy}^{(q)}, a_{yx}^{(q)}, a_{yy}^{(q)}$, respectively. Equation (50) can be used in a truncated version of the characteristic determinant (33) to find the chatter limit.

IV Evaluation of the Chatter Stability Limit

The chatter limit in milling can be determined by solving the characteristic equation of the closed loop milling system, i.e., Eqs. (39) or (33) resulting from single frequency and multi-frequency solutions, respectively. The unknowns in these equations are the chatter frequency ω_c and the axial depth of cut a_{lim} for the defined number of teeth N, radial depth of cut k, spindle speed Ω and milling force constants K_r and K_t. As the characteristic determinants have imaginary and real parts, two unknowns, i.e., ω_c and a_{lim}, can be solved. For the single frequency solution, analytical determination of the chatter limit is possible by obtaining a relationship between the chatter frequency and the spindle speed, which is given in this section. For the multi-frequency solution, a truncated version of Eq. (33) must be used. Such an analytical relationship cannot be obtained for multi frequency solution for which a numerical procedure must be used. However, the numerical examples will show that the single and multi-frequency solutions give almost the same results. Therefore, the following eigenvalue equation is to be considered:

$$\det\,[[I] + \Lambda[G_0(i\omega_c)]] = 0 \quad (52)$$

where the eigenvalue Λ is as follows:

$$\Lambda = -\frac{N}{2\pi}\alpha(1 - e^{-i\omega_c T}) = -\frac{N}{4\pi}K_t\Delta z(1 - e^{-i\omega_c T}) \quad (53)$$

It should be noted that axial depth of cut is equal to $a = m\Delta z$, where Δz and m are the thickness and number of axial elements, respectively. At the limit of stability $a_{lim} = m\Delta z_{lim}$. a_{lim} cannot be directly obtained from Eq. (53) as it does not appear explicitly, but Δz does. It should be noted that for a single axial element case, a_{lim} is equivalent to Δz_{lim} which is obtained from Eq. (53). The procedure to determine the chatter limit is explained by numerical examples in the second part of the paper (Budak and Altintas) and briefly described as follows.

In the formulation of the dynamic milling forces, the variation of the end mill and the workpiece dynamics in the axial direction were modeled by dividing the total axial depth to a number of elements. The element thickness Δz is selected depending on how strong the variations of the dynamics of structures in the axial direction are, and the available modal test data or Finite Element solutions. The difficulty in Eq. (52) is that before the critical axial depth of cut can be determined, the number of elements in the axial direction, m, must be known to construct the matrix $[G_0]$ which contains the oriented transfer functions of the cutter and workpiece, respectively. Therefore, the solution

has to be started with a guess value of m or $\varepsilon = m2\pi$. Then, Eq. (52) should be solved again to determine the new value of the critical depth. This procedure is illustrated on a plane milling example given in Part II (Budak and Altintas). It is realized that a critical radial depth of cut a_{lim} for chatter stability can also be determined from the same equation if the axial depth of cut is specified. The radial depth of cut is implicitly contained in the elements of $[A_0]$ as it determines the start or exit angles (ϕ_{st}, ϕ_{ex}).

The analysis of chatter frequency-spindle speed relation is given in the following in order to solve the chatter stability expressions. The critical axial depth of cut in terms of the element thickness can be obtained from Eq. (53) as

$$\Delta a_{lim} = -\frac{\Lambda}{\frac{N}{4\pi} K_t (1 - e^{-i\omega_c T})} \tag{54}$$

Substituting $\Lambda = \Lambda_R + i\Lambda_I$ and $e^{-i\omega_c T} = \cos\omega_c T - i\sin\omega_c T$ in Eq. (54)

$$\Delta a_{lim} = -\frac{4\pi}{NK_t} \frac{\Lambda_R + i\Lambda_I}{[1 - (\cos\omega_c T - i\sin\omega_c T)]} \tag{55}$$

from which the real and imaginary parts are separated as follows:

$$\Delta a_{lim} = -\frac{4\pi}{NK_t}\left[\frac{\Lambda_R(1 - \cos\omega_c T) + \Lambda_I \sin\omega_c T}{(1 - \cos\omega_c T)^2 + \sin^2\omega_c T} + i\frac{\Lambda_I(1 - \cos\omega_c T) - \Lambda_R \sin\omega_c T}{(1 - \cos\omega_c T)^2 + \sin^2\omega_c T}\right] \tag{56}$$

Δa_{lim} is a real number, then the imaginary part of Eq. (56) must vanish:

$$\Lambda_I(1 - \cos\omega_c T) - \Lambda_R \sin\omega_c T = 0 \tag{57}$$

or,

$$\alpha = \frac{\Lambda_R}{\Lambda_I} = \frac{1 - \cos\omega_c T}{\pm\sqrt{1 - \cos^2\omega_c T}} \tag{58}$$

One of the solutions of Eq. (58) is the trivial solution of $\omega_c T = 0 = 2k\pi$ which corresponds to the case of no regeneration. The nontrivial solution is

$$\cos\omega_c T = \frac{1 - \alpha^2}{1 + \alpha^2} \tag{59}$$

or,

$$\omega_c T = \cos^{-1}\left(\frac{1 - \alpha^2}{1 + \alpha^2}\right) + 2k\pi \tag{60}$$

Equation (60) defines a relationship between the chatter and the tooth frequencies. This equation is the same as the general form of the regeneration expression:

$$2\pi k + \varepsilon = \omega_c T \tag{61}$$

where k is the largest possible integer such that $\varepsilon < 2\pi$. In other words, there are k full vibration cycles and a fraction of 2π of a cycle between the subsequent passes at the same point on the cut surface. In this case,

$$\varepsilon = \cos^{-1}\left(\frac{1 - \alpha^2}{1 + \alpha^2}\right) \tag{62}$$

The following equation for Δa_{lim} is obtained if Eq. (59) is substituted into the real part of Eq. (56) (imaginary part vanishes):

$$\Delta a_{lim} = -\frac{2\pi\Lambda_R}{NK_t}(\varepsilon + 1/\alpha) \tag{63}$$

or,

$$\Delta a_{lim} = -\frac{\pi}{NK_t\Lambda_R}(\Lambda_I^2 + \Lambda_R^2)$$

Therefore, Λ must always be on the left-hand side of the complex plane ($\Lambda_R < 0$) as depth of cut is a positive number. It should be noted that it is easier to determine the tooth period T from Eq. (61) when the chatter frequency ω_c is specified whereas the reverse requires the solution of Eq. (60) which is implicit in ω_c. Therefore, the elemental critical depth of cut is solved from Eq. (63) for different chatter frequencies, i.e., by sweeping the frequencies around the significant structural modes of the dynamic milling system. Then, the corresponding spindle speeds ($n = 60/NT$) are obtained from Eq. (60) for different stability lobes ($k = 1, 2, 3, \ldots$). As explained in the beginning of this section, the corresponding chatter limit can be determined as $a_{lim} = m\Delta a_{lim}$. In general, the value of the eigenvalue Λ can only be determined by numerically solving the eigenvalue problem defined in Eq. (52). It should be noted that this is the only part which requires a numerical solution. However, this is necessary only for the most general case of the milling stability. As shown in Part II (Budak and Altintas), the numerical eigenvalue solution is not necessary for most of the practical cases. These are the cases where the variation of the cutter and workpiece dynamics in the axial direction can be neglected, i.e., $m = 1$, which is generally the case for face milling or high speed end milling operations with a small depth of cut.

When computing the value of ε, it should be noted that $\varepsilon' = 2\pi - \varepsilon$ is also a solution to the ($\cos^{-1}$) function given in Eq. (62). For this, consider the angle defined by the eigenvalue Λ in the complex plane,

$$\varphi = \tan^{-1}\frac{\Lambda_I}{\Lambda_R} = \tan^{-1}\frac{1}{\alpha} \tag{64}$$

By substituting $\alpha = 1/\tan\varphi$ into Eq. (59), the following is obtained:

$$\cos\omega_c T = -\cos 2\varphi \tag{65}$$

The solution to the above equation is

$$\omega_c T = (\pi \pm 2\varphi) + 2k\pi \tag{66}$$

Substituting the possible solutions for $\omega_c T$ given in the above equation into Eq. (57) and considering

$$\omega_c T = \varepsilon + 2k\pi, \tag{67}$$

the solution can be found as follows:

$$\varepsilon = \pi - 2\varphi \tag{68}$$

It should be noted that as $\Lambda_R < 0$ always, then $\varphi \in (\pi/2 - 3\pi/2)$.

Therefore, by using the milling stability formulation developed in this paper, the relationship between the chatter frequency and the spindle speed in milling is obtained. The complete analytical solution of stability lobes for a multi-degree-of-freedom cutter-workpiece assembly is therefore possible with the method presented here.

Example: Stability Lobes for a 2-DOF End Milling System. The analytical stability method is demonstrated on a 2-DOF end milling system considered by Weck et al. (1994).

The dynamic properties of the 3-flute end mill, lumped at the free end of the cutter, were identified as:

	ω_n (Hz)	k (kN/m)	ζ
X	603	9000	0.039
Y	868	5700	0.033

The aluminum workpiece is considered to be rigid compared to the cutter. The stability limits from cutting tests (Weck et al., 1994) and simulations for a half-immersion (up milling) case are shown in Fig. 3. K_t = 600 MPa and K_r = 0.07 are used as given in (Weck et al., 1994), and feed rate was s_t = 0.07 mm/tooth. Time domain simulation results are also shown in the figure in addition to the solutions obtained by the proposed method in this paper. The exact kinematics of milling was employed in the time domain simulations as described in (Altintas et al., 1992). For time domain stability limit predictions, the dynamic milling process has to be simulated at different spindle speeds for varying axial depth of cuts. The stability of the process is judged depending whether the cutting forces and vibration amplitudes increase in time. In general, many revolutions of the cutter have to be considered since chatter vibrations grow slowly due to the nature of regeneration. The accuracy of the simulations also depends on the increment size in the axial depth of cut. Thus, generation of a stability diagram with time domain simulations take extremely long computation time, usually in the order of hours (depending on the time step and axial depth increment sizes), on workstations. The stability limit predictions by using single frequency (analytical) and multi frequency (up to third order) methods are also shown in Fig. 3. As it can be seen from the figure, zero and higher order solutions give almost the same results, which is expected as described in the stability analysis. An iterative solution has to be used for multi-frequency solution as the explicit relationship between the spindle speed and the chatter frequency obtained for the single frequency solution (Eq. (40)) cannot be used directly. The iterations are started using the analytical solution until the convergence is obtained. The solution usually converges in a few iterations. The complete stability diagram can be generated in less than 10 seconds on a 486DX2 PC. In addition, these solutions are in excellent agreement with the time domain simulations as it can be seen from the figure. The stability lobes in the figure are shown for high spindle speeds in order to demonstrate the agreement among the single and multi frequency solutions, and the time domain results, for the cases where the tooth passing frequency is close to the natural frequency. The general form of the experimental stability data, which is available only in relatively low cutting speeds, is in good agreement with the predictions. The effect of the process damping can be seen in the experimental chatter limits especially at the slow speeds. The average difference between the experimental data and the predictions is less than 1 mm and the discrepancy can be attributed to process damping which is not considered in the predictions. However, the difference is expected to be much smaller for higher speeds where the effect of process damping decreases. This example demonstrates that the developed model can be used for fast and accurate predictions of the stability limits in milling. Also, it is shown that the analytical or single frequency solution gives the same results with the multi frequency solution. In the second part of the paper (Budak and Altintas) the analytical formulation for a 2-DOF milling system is further simplified.

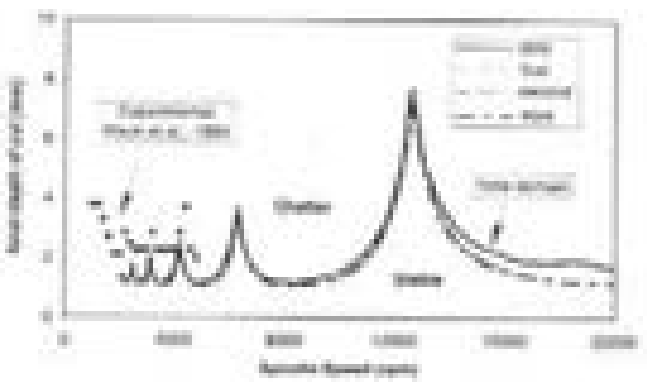

Fig. 3 Analytical, simulation and experimental stability diagrams for a 2-DOF end milling system. Workpiece material: aluminum, cutter: 3 flute, HSS end mill in half immersion up-milling.

V Conclusions

An analytical method is presented in solving the chatter stability problem for end milling operations. The structural dynamics in the plane of cut, as well as variations along the axial direction are considered. A comprehensive formulation of dynamic milling forces is given by modeling the workpiece and cutter as multi-degree-of-freedom structures. The governing equation of dynamic milling contains periodically varying terms due to the rotating directional coefficients between the chip thickness and the modal directions. The stability analysis is performed by expanding the periodic matrix into Fourier series, and using the basic physical properties of dynamic cutting and regeneration mechanism. It is shown that, when a single frequency is considered as representing the dynamic response of the milling system, it is possible to obtain an analytical solution for the stability lobes. The model predictions are verified by experimental results and time domain simulations. It is demonstrated that the analytical-single frequency solution gives almost identical results to the multi frequency solutions. The analytical solution eliminates the extremely long time domain simulations for the stability lobes. The application of the general formulation developed here on some common face and end milling operations with different structural dynamics configurations is illustrated in the second part of the paper (Budak and Altintas).

Acknowledgment

This work was sponsored by National Science and Engineering Research Council of Canada and Pratt & Whitney Canada Inc. under collaborative research grant programs 5-80668 and 5-54085.

References

Altintas, Y., Montgomery, D., and Budak, E., 1992, "Dynamic Peripheral Milling of Flexible Structures," ASME Journal of Engineering for Industry, Vol. 114(2), pp. 133–145.

Budak, E., and Altintas, Y., 1994, "Analytical Prediction of Chatter Stability in Milling—Part II: Application of the General Formulation to Common Milling Systems," published in this issue, pp. 31–36.

Budak, E., 1994, Mechanics and Dynamics of Milling Thin Walled Structures, PhD thesis, The University of British Columbia.

Chen, S. G., Chen, A. G., and Rivin, E., 1993, "Computational Stability Analysis of Chatter in Turning," 1993 ASME Winter Annual Meeting, Symposium on Microstructures, ASME DE-Vol. 59/PED Vol. 65, pp. 107–111.

Hahn, R. S., Koller, R., and Lang, G. W., 1968, "A Stability Algorithm for a Special Case of the Milling Process," ASME Journal of Engineering for Industry, pp. 322–324.

Koenigsberger, F., and Tlusty, J., 1967, Machine Tool Structures Vol. 1, Stability Against Chatter, Pergamon Press.

Lee, A. C., and Liu, C. S., 1991a, "Analysis of Chatter Vibration in the End Milling Process," International Journal of Machine Tool Design and Research, Vol. 31(4), pp. 477–478.

Liu, A. C., Liu, C. S., and Chiang, R. T., 1991b, "Analysis of Chatter Vibration in a Cutter-Workpiece System," International Journal of Machine Tool Design and Research, Vol. 31(2), pp. 223–234.

Magnus, W., and Winkler, K., 1966, Hill's Equation, Wiley, N.Y.

Merritt, H. E., 1965, "Theory of Self-Excited Machine Tool Chatter," ASME Journal of Engineering for Industry, Vol. 87, pp. 447–454.

Shin, J. and Tlusty, T., 1993, "A New Theoretical Approach for the Prediction of Machine Tool Chatter in Milling," ASME Journal of Engineering for Industry, Vol. 115, pp. 1–8.

n°1216

Analytical Prediction of Chatter Stability in Milling—Part II: Application of the General Formulation to Common Milling Systems

E. Budak[1]

Y. Altintaş

Department of Mechanical Engineering,
The University of British Columbia,
Vancouver, B.C., Canada V6T 1Z4

The general formulation for the milling chatter prediction developed in Part I of the paper is applied to common milling systems. Three cases are considered: a workpiece with single-degree-of-freedom, a face milling cutter with two-degree-of-freedom, and peripheral milling of a considered thin web. The general milling stability formulation is further simplified for the less complicated models. For each case, an analytical expression which explicitly relate the chatter limit to the milling conditions and tool workpiece dynamics are derived. The analytical predictions are compared with numerical and time domain solutions proposed by previous research. It is shown that the proposed method can accurately predict the chatter limits in milling and thus eliminates the time consuming numerical solutions.

1 Introduction

Recent literature indicate that the chatter vibrations in single point turning and boring operations may be actively controlled by high bandwidth actuators and linear drives (Altintaş and Yuen, 1994). However, chatter in milling operations can be suppressed either at high speeds (Smith and Delio, 1989) by an on-line sensor-based automatic spindle speed regulation, or by selecting chatter free depth of cuts and speeds at the process planning stage with the aid of stability lobes which are generated using time domain simulations (Weck et al., 1994; Smith and Tlusty, 1990). In this paper, the analytical prediction of stability lobes presented in Part I (Budak and Altintaş) of the paper is applied to some common dynamic milling systems studied in the literature using other techniques and time domain simulations.

The general stability lobe formulation developed in the first part of the paper (Budak and Altintaş) considers the dynamic displacements of the milling cutter and workpiece in x and y directions, and the variation of their dynamic characteristics in the axial z direction. The variation of the dynamics in the axial direction is important in milling very flexible workpieces such as long and thin webs, and may affect the stability limit (Altintaş et al., 1992). However, for most of the milling systems where the dynamics can be lumped at a cutting point, this variation is negligible. In this part of the paper, several common milling systems are modeled and the developed formulation is applied to predict chatter limits. The computed results are verified with numerical and time domain simulation values found in the literature (Opitz et al., 1968; Sridhar et al., 1968b; Minis et al., 1993; Smith and Tlusty, 1993).

The stability limit and phase (or spindle speed) formulas developed in Part I (Budak and Altintaş) require the solution of the eigenvalue Λ for the characteristic equation $[[J] + \Lambda[G_0(i\omega_c)]] = 0$. For the general multi-degree-of-freedom case, the eigenvalue problem must be solved using numerical methods, which is the only numerical part in the formulation. For the first two cases considered in this part of the paper, the solutions can be obtained completely analytically, since the characteristic equation has only quadratic terms. The analytical solution provides direct relationships between the milling conditions, stability limit and chatter frequency, and contributes to the understanding of dynamic milling process-structure interaction.

2 Milling of a Flexible Workpiece-Single Axial Element

Consider the single-degree-of-freedom dynamic milling model shown in Fig. 1. This model represents the milling of a flexible workpiece with a relatively rigid cutter. It should be noted that, although the workpiece is modeled by using single axial element, it can have more than one vibration mode in the considered direction. The peripheral milling of thin walled components can also be analyzed by this model if the considered axial depth of cuts are small so that the dynamics of the workpiece can be assumed constant within the cutting depth.

The system shown in Fig. 1 has single axial element, i.e., $m = 1$, $\Delta z_{1m} = a_{1m}$. For the single frequency solution, the eigenvalue equation (Part I-52) in (Budak and Altintaş) becomes:

$$1 - \frac{N}{4\pi} K a_{1m} [1 - e^{-i\omega_c T/2}] a_{1m} G_y(i\omega_c) = 0 \qquad (1)$$

where a_{1m} is the directional coefficient given in Part I (Part I-Eq. (47), Budak and Altintaş):

$$a_{1m} = \frac{1}{2}[-\cos 2\Phi - 2K\Phi + K \sin 2\Phi]_{\Phi_{st}}^{\Phi_{ex}} \qquad (2)$$

G_y is the transfer function of the workpiece in the y direction:

$$G_y(i\omega_c) = \frac{\omega_{ny}^2 / k_y}{\omega_{ny}^2 - \omega_c^2 + 2\zeta_y \omega_{ny} \omega_c i} \qquad (3)$$

where k_y, ζ_y and ω_{ny} are the stiffness, damping ratio, and undamped natural frequency of the workpiece in the y direction. If the workpiece has more than one vibration mode in this direction, then the transfer function G_y can be determined by

[1] Currently with Pratt and Whitney Canada, 1000 Marie-Victorin, Longueuil, Quebec, Canada, J4G 1A1.

Contributed by the Dynamic Systems and Control Division for publication in the JOURNAL OF DYNAMIC SYSTEMS, MEASUREMENT, AND CONTROL. Manuscript received by the DSCD January 6, 1995. Associate Technical Editor: Yau-Chu Tsao.

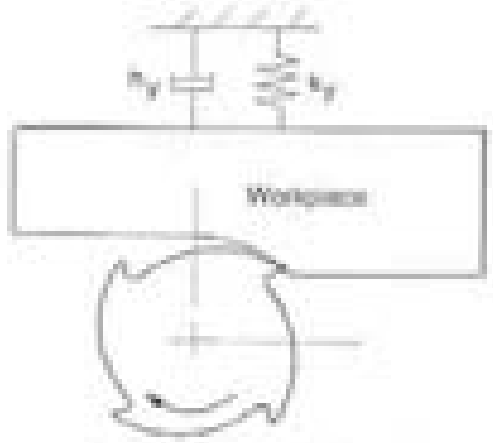

Fig. 1 Single-degree-of-freedom milling system model

modal superposition. From Eq. (1), the chatter limit is obtained as

$$a_{lim} = \frac{1}{\frac{N}{2\pi} K_t G_y(i\omega_c)(1 - e^{-i\omega_c T})} \tag{4}$$

As a_{lim} is a real number, the imaginary part of the complex term $G_y(i\omega_c)(1 - e^{-i\omega_c T})$ must vanish. Hence, the imaginary parts of $G_y(i\omega_c)e^{-i\omega_c T}$ and $G_y(i\omega_c)$ should be equal to each other. This is possible when the real parts have opposite signs (see Fig. 2) resulting in

$$G_y(i\omega_c)(1 - e^{-i\omega_c T}) = 2\mathrm{Re}[G_y(i\omega_c)] \tag{5}$$

The real part of the transfer function $G_y(i\omega_c)$ is as follows:

$$\mathrm{Re}[G_y(i\omega_c)] = \frac{1}{k_s}\frac{1 - d_c^2}{(1 - d_c^2)^2 + 4\zeta^2 d_c^2} \tag{6}$$

where $d_c = \omega_c/\omega_n$. Substituting (5) in Eq. (4)

$$a_{lim} = \frac{1}{\frac{N}{2\pi} K_t \mathrm{Re}[G_y(i\omega_c)]} \tag{7}$$

From Fig. 2, the phase ϵ is obtained as in the orthogonal cutting chatter stability theory:

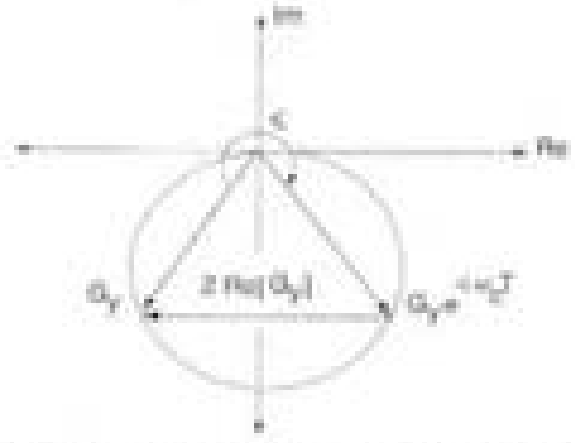

Fig. 2 The phase angle and transfer function at the chatter stability limit. In milling, chatter frequency may be higher or lower than the modal frequency depending on the cutting conditions.

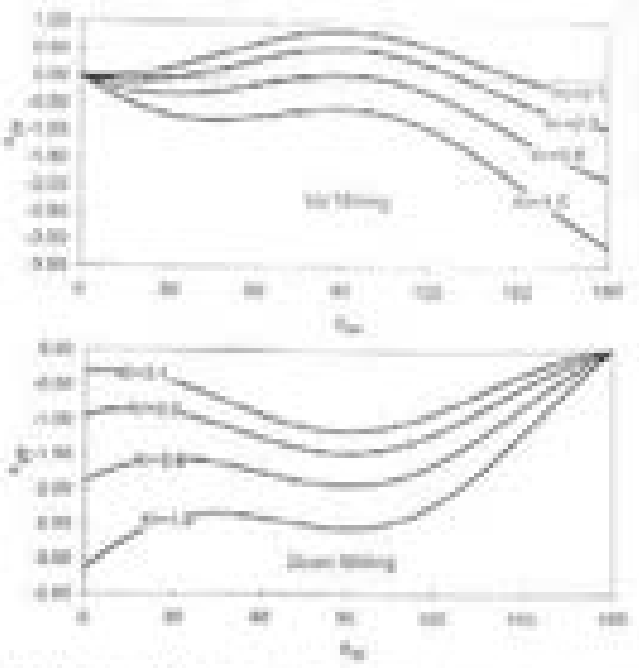

Fig. 3 Variation of the directional milling coefficient a_{lim} with the immersion angle in up and down milling. The sign and magnitude of the directional coefficients determine the chatter frequency and stability limit, respectively.

$$\epsilon = 2\pi - 2\tan^{-1}\frac{d_c^2 - 1}{2\zeta d_c} \tag{8}$$

Then, the spindle speeds (n) corresponding to the considered chatter frequency ω_c in different lobes (k) can be found from

$$2\pi k + \epsilon = \omega_c T \tag{9}$$

where $n = 60/(NT)$.

The equations derived for milling here are similar to the stability condition developed by Tlusty (1967) for single tooth cutting with constant directional coefficients, e.g., turning and boring. Equation (7) suggests that the chatter frequency can be smaller or higher than the natural frequency depending on the signs of the directional milling coefficient a_{lim}. If $a_{lim} > 0$, then $\mathrm{Re}[G_y(i\omega_c)]$ must be positive, i.e., $\omega_c < \omega_n$, in order to have $a_{lim} > 0$, and vice versa. In the classical orthogonal cutting stability theory of Tlusty (1967), the chatter frequency is always larger than the modal frequency. This is because of the presumed positive direction for the feed cutting force which can only be negative for large and impractical rake angles (due to an increased component of the rake face force in the feed direction). However, in milling, the directional coefficients are not constant, $a_{xx}, \ldots, a_{xy}$ represent averaged directional milling coefficients, and depending on the radial immersion of the cutter and K_r, their sign may change. Minis et al. (1990) showed that even in turning, the chatter frequency at the limit of stability can be smaller or larger than the modal frequency depending on the orientation of the tool holder (right or left-handed), thus the transfer function. The variations of a_{lim} with the immersion angle for up and down milling and different K_r values are shown in Fig. 3. a_{lim} is always negative for down milling, thus the chatter frequency is always higher than the natural frequency of the structure, whereas in up milling, it depends on the exit angle. a_{lim} is smaller for up milling resulting in higher stability limits. This is due to the fact that, in up milling, the components of the tangential and radial forces in the normal y direction are in the opposite directions. Budak and Altintas (1994b) used this feature in selecting an optimal radial depth of cut to minimize tool deflections and dimensional surface errors. As it can be seen from Fig. 3, the variation of the directional coefficient

Fig. 4 A single-degree-of-freedom system: Comparison of the predicted chatter limit with the published data (Minis and Yanushevsky (1993), analog data is from Opitz (1968), and Sridhar et al. (1968b))

a_{lim} and thus the stability limit a_{lim} with the radial immersion is not linear. These graphs can be used to determine the optimal radial depth of cuts for chatter free milling.

Example: Milling of a SDOF Structure. The stability formula developed in this section is applied to a milling operation investigated by Opitz (1968), Sridhar et al. (1968), and Minis et al. (1993). The flexibility of the workpiece in the x direction is represented by a single-degree-of-freedom system with the following parameters:

$$k_x = 7.132 \times 10^7 \text{ N/m } (39700 \text{ lbf/in}), \ \zeta_x = 0.0417$$

$$\omega_{n_x} = 355 \text{ rad/s}$$

A face milling cutter with $N = 10$ straight teeth is used, and the start and exit angles are 67 and 139 deg, respectively. $K_r = 0.577$ and a_{lim} is calculated from Eq. (Part I-45) as $(-1/\lambda)$. Equation (7) (a_{xx} and G_x are to be used in place of a_y and G_y as the workpiece is flexible in the feed direction) was used to calculate the stability limit for different values of chatter frequency ω_c. Then, the corresponding spindle speeds are found from Eq. (Part I-61). Stability lobes are shown in Fig. 4 in terms of the product of critical depth of cut a_{lim} and the tangential cutting force coefficient, i.e., $K_t = K_t(1 + K_r^2)$ as in Sridhar et al. (1968). Also shown in Fig. 4 is the data from (Minis and Yanushevsky (1993) and Sridhar et al. (1968)). Minis et al. (1993) iteratively determined the stability limit for a given spindle speed by examining the stability of the system for different axial depths. They used periodic system theory in formulating the milling stability problem as explained in Part I of the paper (Budak and Altintas, 1995). Sridhar et al. (1968) used the analog simulation data from Opitz (1968) to compare with their numerical stability solution results. All these solutions, which use different approaches, show excellent agreement except around the first stability lobe. Around the peak stability points, the chatter frequencies are very close to the natural frequency of the structure since $\text{Re}[G(i\omega_c)] \to 0$ as $\omega_c \to \omega_{n_x}$. At these frequencies the variation of $\text{Re}[G(i\omega_c)]$ with the frequency or spindle speed is quite steep, and therefore a fine spindle speed or frequency resolution is necessary for accurate results. It should be noted that the only analytical solution is the method proposed in this paper. The resolution can be made as fine as required without increasing the computation time significantly. The numerical solution procedures used in Opitz (1968) and Minis and Yanushevsky (1993) may have resulted in the differences around the peaks.

III Milling of a Flexible Structure With a Flexible End Mill-Single Axial Element

Consider the milling system model shown in Fig. 5. This is the most general case of a milling system where only one axial element is considered, i.e., there is no variation in the dynamics of the structure along the axial direction. As in the previous case, the cutter and workpiece can have more than one vibration mode in the two considered orthogonal directions, x and y. Then, the general stability equation takes the following (Budak and Altintas, 1998) form:

$$\det\left([I] + \Lambda\begin{bmatrix} a_{xx}a_{yx} \\ a_{xy}a_{yy} \end{bmatrix}\begin{bmatrix} G_x(i\omega_c) & 0 \\ 0 & G_y(i\omega_c) \end{bmatrix}\right) = 0$$

where $a_{xx}, \ldots, a_{yy}$ are given in Eq. (Part I-45). $G_x = G_{x_w} + G_{x_c}$, G_{x_w} and G_{x_c} are the cutter and workpiece transfer functions which may include contributions of more than one vibration mode. The cross-transfer functions G_{xy} and G_{yx} have been neglected for the sake of algebraic simplicity. From Eq. (10) the following quadratic equation is obtained for Λ:

$$a_0\Lambda^2 + a_1\Lambda + 1 = 0 \tag{11}$$

where

$$a_0 = G_x(i\omega_c)G_y(i\omega_c)(a_{xx}a_{yy} - a_{xy}a_{yx})$$
$$a_1 = a_{xx}G_x(i\omega_c) + a_{yy}G_y(i\omega_c) \tag{12}$$

Then, the eigenvalues Λ are obtained as:

$$\Lambda = -\frac{1}{2a_0}(a_1 \pm \sqrt{a_1^2 - 4a_0}) \tag{13}$$

The critical axial depth of cut can be obtained by substituting Λ into Eq. (Part I-61):

$$a_{lim} = -\frac{2\pi\Lambda_r}{NK_t}(\varepsilon + 1/\varepsilon) \tag{14}$$

where $\varepsilon = \Lambda_i/\Lambda_r$. Corresponding spindle speed ($n = 60/NT$) to a considered chatter frequency can be found from Eqs. (Part I-64), (Part I-67), and (Part I-68) as:

$$\omega_c T = \varepsilon + 2k\pi$$

where

$$\varepsilon = \pi - 2\psi$$

and

$$\psi = \tan^{-1}\frac{\Lambda_i}{\Lambda_r} = \tan^{-1}\frac{1}{\varepsilon}$$

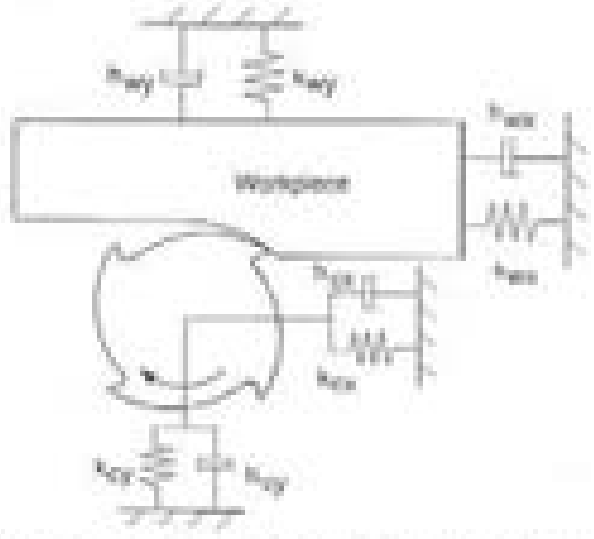

Fig. 5 Flexible workpiece and flexible cutter in feed (x) and normal (y) directions

Fig. 6 Analytical, multi frequency and time domain stability limit predictions for a case analyzed by Smith and Tlusty (1990)

Example: Milling a Rigid Workpiece With 2-DOF End Mill. A 2 DOF milling system example is taken from Smith and Tlusty (1990). This is a half immersion up milling of an aluminum workpiece by a 4 in. diameter shell mill with 8 teeth. The modal properties of the cutter are given as follows:

	Mode	ω_n (Hz)	k (N/m)	ζ
X	1	280	2.26×10^6	0.12
	2	599	5.54×10^7	0.04
Y	1	150	2.13×10^6	0.1
	2	348	2.14×10^7	0.1

The results of the analytical method predictions (K_t = 1500 MPa and K_r = 0.3) and the time domain simulations performed by Smith and Tlusty (1990) are shown in Fig. 6. A multi-frequency solution is also included by considering the first harmonic term in the Fourier series, i.e., by using Eq. (Part I-34). The eigenvalue of this equation is numerically solved by using the spindle speed (corresponding to a specific chatter frequency) obtained from the analytical solution, for the first iteration. Then, the new values of the chatter limit and spindle speed are determined by using the calculated eigenvalue. The new spindle speed is used to calculate the eigenvalue again until a convergence is obtained. During the solutions it was observed that the convergence is usually obtained in one cycle. As it can be seen from the figure, the single frequency approximation, which provides a complete analytical solution without any iterations, is in excellent agreement with the time domain simulations and multi frequency solution. As explained in Part I of the paper (Budak and Altintas, 1995) the single frequency solution corresponds to taking the average term of the cutting force coefficients in the Fourier series expansion. Although both analytical and time domain solutions give almost identical results, there is a big difference in the computation times. The proposed analytical solution, which can even be performed on a spreadsheet software, takes less than a minute on a PC-486 (66 MHz) to simulate the complete stability diagram. For the time domain solutions, on the other hand, sophisticated simulation programs need to be developed, and the computation time is usually in the order of hours.

IV Milling of a Flexible Structure With a Rigid End Mill—Varying Dynamics in Axial Direction

In this section, the application of the general stability formulation to the milling of flexible workpieces is given by considering the variation of the workpiece dynamics in the axial direction. The workpiece is assumed to be modelled by discrete masses lumped along the cutter—workpiece contact zone in y direction. The cutter is assumed to be rigid in comparison to the very flexible workpiece. For this case, the stability Eq. (Part I-32) becomes:

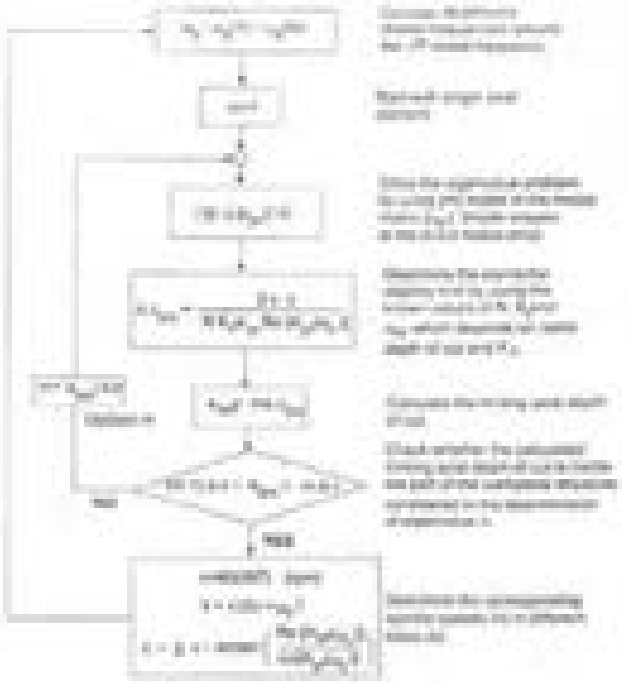

Fig. 7 Stability limit calculation algorithm for flexible workpieces with varying dynamics in the axial direction

$$\det\left([I] + \frac{N}{4\pi} a_0 (1 - e^{-i\omega_c T}) \sum_{j=1}^{m} [A_j] G_j(i\omega_c)\right) = 0 \quad (15)$$

The transfer function of the workpiece in the y direction can be obtained by modal superposition as:

$$[G_j(i\omega_c)] = \sum_{r=1}^{n} [\alpha_{jr}] H_r(i\omega_c) \quad (16)$$

where:

$$H_r(i\omega_c) = \frac{1}{\omega_{n_r}^2 - \omega_c^2 + 2i\zeta_r\omega_{n_r}\omega_c} \quad (17)$$

and $[\alpha_{jr}] = [a_{jr}]\,[a_{jr}]^T$ is the j^{th} undamped modal matrix of the workpiece, normalized for unity modal mass (the structure is assumed to be proportionally damped). The stability diagrams for flexible workpiece milling can be generated by using the general stability Eq. (Part I-63). However, the formulation is further simplified if the modes of the workpiece are well separated. In this case, the stability analysis can be performed around the most flexible mode of the structure by neglecting

Fig. 8 Predicted stability lobes for the peripheral milling of a cantilevered thin plate. Cutting conditions: Ti6Al4V plate with height = 64 mm, length = 63.5 mm and uncut thickness = 3.8 mm. Radial depth of cut is b = 0.508 mm in down milling mode, with a 4 fluted 19.05 mm dia 30 deg helical carbide end mill. Identified cutting constants are K_t = 1500 MPa and K_r = 0.3.

Fig. 9 Predicted stability lobes for the peripheral milling of the cantilevered thin plate considered in Fig. 8. Cutting conditions: Radial depth of cut is b = 0.635 mm in down milling mode, with a 6 fluted 19.05 mm dia 30 deg helical carbide end mill.

the contributions of the other modes. Then, for the r^{th} mode, Eq. (15) becomes:

$$\det[[I] - \Lambda[a_{rr}]] = 0 \tag{18}$$

where

$$\Lambda = \frac{N}{4\pi} K_t \Delta z_{lim} (1 - e^{-i\omega_r T}) [a_{jr}] [A_{rr}] (\Delta z_{lim}) \tag{19}$$

The imaginary parts in Eq. (19) must vanish to obtain a real Δz. The eigenvalue Λ is a real number as the $[a_{jr}]$ in equation (18) is a real matrix. Then, similar to Eq. (7), the following is obtained for the critical depth of cut in terms of the elemental thickness Δz_{lim}:

$$\Delta z_{lim} = \frac{\Lambda}{\frac{N}{2\pi} K_t a_{jr} Re[A_{rr}(\Delta z_{lim})]} \tag{20}$$

As explained in Part I, the critical depth of cut is obtained as $a_{lim} = m\Delta z_{lim}$, m is the number of axial elements. For an arbitrary m and axial depth of cut $a = m\Delta z$, if a_{lim} is $a + \Delta z$ or $a_{lim} < a - \Delta z$, the new value of m has to be determined as

$$m' = a_{lim}/\Delta z = m\Delta z_{lim}/\Delta z \tag{21}$$

The solution is started with $m = 1$. The procedure is outlined in Fig. 7 and the method is discussed with a plate milling example in the following.

Example: Peripheral Milling of a Cantilevered Thin Plate. The structural and cutting mechanics models investigating the static and dynamic milling of such cantilevered thin plates were presented by the authors (Altintas et al., 1992; Budak and Altintas, 1994a). The plate is modelled by the Finite Element method, and the static and dynamic interaction between the plate and cutter are studied at each elemental contact zones in time domain simulations. It was discussed in Altintas et al. (1992) that the time domain simulation of such a slender and long structure with a large axial and very small radial depth of cuts is not only computationally expensive, but leads to frequent numerical instabilities. The plate milling stability is solved here by using the proposed analytical technique.

Stability limits in milling a cantilever plate (Ti-6Al-4V) with dimensions (63.5 × 44 × 3.8 mm) is simulated. The 19.05 mm diameter end mill, which is assumed to be rigid, has 4 flutes, and is used in the down milling mode to finish the plate surface. As frequently experienced in the finishing of very flexible components, a very small radial depth of cut, b = 0.0508 mm with ϕ_s = 175 deg (this allows relatively high critical depth of cuts so that more than one axial element is in cut), used in the simulations to show the effects of mode shapes on the stability limits (K_c = 1500 MPa, K_r = 0.7). The Finite Element method was used to determine the normalized modal vectors and frequencies of the plate. Plate is divided into 16 axial elements in the cutting zone with Δz = 2.75 mm. Structural damping ratio of 0.05 was used. The first three modal frequencies of the plate are 1667, 3057, and 7074 Hz. Figure 8 shows the simulated stability lobes around the first dominant bending mode (1667 Hz). It should be noted that for the bending mode, the mode shape at the cutter location (along the cutter axis) does not vary along the feed direction (the rotational mass is negligible for this case). However, in general, mode shapes vary in the feed direction (e.g., for torsional modes of the plate), in which case the simulations have to be repeated at number of locations along the feed direction. The normalized modal values (for unity modal mass) for the considered axial depth range shown in Fig. 8 are $[a_{jr}]^T$ = {9.90, 9.65, 8.14, 7.28, 6.42, 5.60, . . . , 0.12,

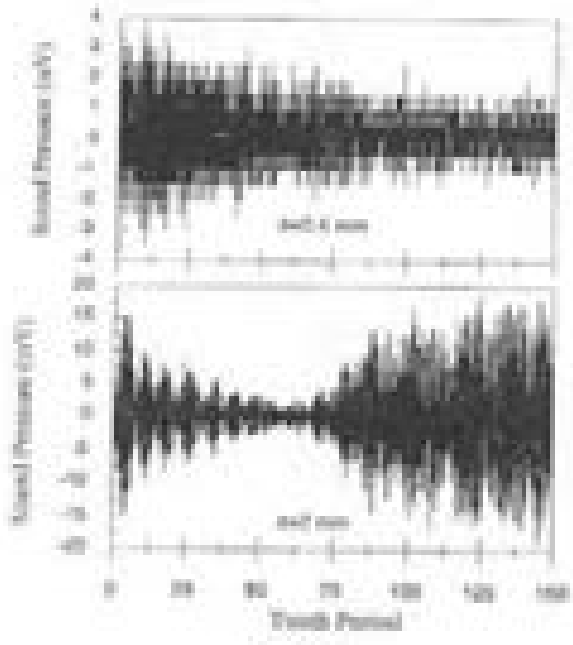

Fig. 10(a)

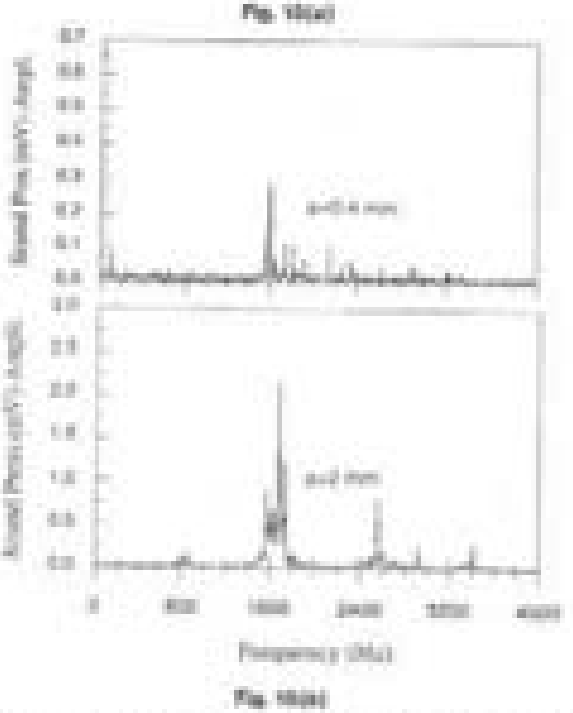

Fig. 10(b)

Fig. 10 Measured sound signals (a) and spectrums (b) from stable (a = 0.4 mm) and unstable (a = 2 mm) plate milling tests, see Fig. 9 for the cutting conditions.

0). Figure 8 shows that, compared to the single element solution, the multi element solution gives higher critical depth of cut predictions (about 50 percent around the high stability lobe shown) as it considers the variation in the workpiece dynamics in the axial direction. In this case, the first bending mode of the plate has the highest displacement at the free end, which decreases towards the fixed end. Note that the discrete modeling of the workpiece dynamics results in discontinuities in the stability diagram as the dynamic characteristics are assumed to be constant within the axial elements.

In order to demonstrate the accuracy of the stability limit predictions, another plate milling example is given, by using the same plate considered in the previous case. Figure 9 shows the stability diagram for the peripheral milling of the plate at the beginning of the cut in the feed direction. The plate is finished by using a 8 flutted, 19.05 mm diameter, 30 deg helical carbide end mill in down milling mode. The radial depth of cut is $b = 0.325$ mm or $\phi_{st} = 165$ deg. Feed per tooth of $c_t = 0.008$ mm is used. As it can be seen from the diagram, compared to the previous example, the stability limits are extremely small in this case, due to increased radial depth of cut and number of flutes. Because of very small axial immersions, the variation of the plate dynamics in the axial direction is neglected, and the analytical solution given by Eq. (7) is used for the stability limits. Sample cutting experiments were conducted to check the validity of the plate milling stability analysis. The plate is cut at $n = 6500$ rev/min with the same cutting conditions used in stability lobe generation. The vibrations are monitored by a microphone located close to the plate machining zone, and the location of the microphone was fixed during all experiments. Measured sound pressure and its spectrum at two sample experiments at axial depth of cuts $a = 0.4$ mm and $a = 2$ mm are shown in Fig. 10. Excessive chatter vibrations at the first bending mode (1667 Hz) of the plate is quite evident at $a = 2$ mm, which is above the stability pocket limit predicted in Fig. 9. It should be noted that, unlike in the majority of the milling systems, in plate milling the forced vibration amplitudes are quite high, in addition to the chatter vibrations, due to very high flexibility of the plate. Especially at $n = 6500$ rpm, the second harmonic of the milling forces ($= 1733$ Hz) is very close to the first mode of the plate, which results in resonance. Therefore, in order to see the differences between stable and unstable cuts more clearly, two axial depths, one below the stability limit and one well above it are considered.

V Conclusions

In this part of the paper, the general milling chatter formulation developed in Part I is applied to several common milling systems. Analytical solutions are developed for the chatter limit for single and two-degree-of-freedom systems. The effect of the workpiece dynamics variation in the axial direction is demonstrated on a plate milling example. Analytical predictions of the method is compared with numerical and time domain solutions given in the literature. The model can predict the chatter limits fast and accurately. Also, the relations between the cutting conditions, e.g., radial depth of cut, tool geometry, and the chatter limit can be used for process planning of milling operations.

Acknowledgment

This work was sponsored by National Science and Engineering Research Council of Canada and Pratt & Whitney Canada Inc. under a collaborative research grant programs 5-80668 and 5-34065.

References

Altan, O. M., and Tsao, T. C., 1994, "Stability of Turning Processes with Actively Controlled Linear Motor Feed Drives," *ASME Journal of Engineering for Industry*, Vol. 116, pp. 299–307.

Altintas, Y., Montgomery, D., and Budak, E., 1992, "Dynamic Peripheral Milling of Flexible Structures," *ASME Journal of Engineering for Industry*, Vol. 114(2), pp. 137–145.

Budak, E., and Altintas, Y., "Analytical Prediction of Chatter Stability in Milling—Part I: General Formulation," published in this issue pp. 22–30.

Budak, E., and Altintas, Y., 1994a, "Modeling and Avoidance of Static Deformations in Peripheral Milling of Plates," *International Journal of Machine Tools and Manufacture*, Vol. 34(7), pp. 459–476.

Budak, E., and Altintas, Y., 1994b, "Peripheral Milling Conditions for Improved Dimensional Accuracy," *International Journal of Machine Tools and Manufacture*, Vol. 34(7), pp. 907–918.

Koenigsberger, F., and Tlusty, J., 1967, *Machine Tool Structures—Vol. I: Stability Against Chatter*, Pergamon Press.

Minis, I., Magrab, E. B., and Pandelidis, I. O., 1990, "Improved Methods for the Prediction of Chatter in Turning, Part 3: A Generalized Linear Theory," *ASME Journal of Engineering for Industry*, Vol. 112, pp. 28–35.

Minis, I. and Yanushevsky, T., 1993, "A New Theoretical Approach for the Prediction of Machine Tool Chatter in Milling," *ASME Journal of Engineering for Industry*, Vol. 115, pp. 1–8.

Opitz, H., 1968, "Chatter Behavior of Heavy Machine Tools," Quarterly Technical Report No. 2 AF 61 (052)-916, Research and Technology Division, Wright-Patterson Air Force Base, OH.

Smith, S., and Tlusty, J., 1990, "Update on High Speed Milling Dynamics," *ASME Journal of Engineering Industry*, Vol. 112, pp. 142–149.

Smith, S., and Delio, 1989, "Sensor-Based Control for Chatter-Free Milling by Spindle Speed Selection," *Proceedings of the ASME 1989 Winter Annual Meeting*, Vol. DE pp. 107–114.

Sridhar, R., Hohn, R. E., and Long, G. W., 1968a, "General Formulation of the Milling Process Equation," *ASME Journal of Engineering for Industry*, pp. 317–324.

Sridhar, R., Hohn, R. E., and Long, G. W., 1968b, "A Stability Algorithm for the General Milling Process," *ASME Journal of Engineering for Industry*, pp. 330–334.

Weck, M., Altintas, Y. and Ruo, C. 1994, "CAD Assisted Chatter Free NC Tool Path Generation in Milling," *International Journal of Machine Tool Design and Research*, Vol. 34(6), pp. 879–891.